Available online at www.sciencedirect.com
ScienceDirect
Journal of Solid State Chemistry 180 (2007) 1291–1297
JOURNAL OF SOLID STATE CHEMISTRY
www.elsevier.com/locate/jssc

Preparation and optical properties of silica@Ag–Cu alloy core-shell composite colloids

Jianhui Zhang*, Huaiyong Liu, Zhenlin Wang, Naiben Ming

National Laboratory of Solid State Microstructures, Department of Physics, Nanjing University, Nanjing 210093, China

Received 5 September 2006; received in revised form 22 January 2007; accepted 24 January 2007
Available online 15 February 2007

Abstract

The silica@Ag–Cu alloy core-shell composite colloids have been successfully synthesized by an electroless plating approach to explore the possibility of modifying the plasmon resonance at the nanoshell surface by varying the metal nanoshell composition for the first time. The surface plasmon resonance of the composite colloids increases in intensity and shifts towards longer, then shorter wavelengths as the Cu/Ag ratio in the alloy shell is increased. The variations in intensity of the surface plasmon resonance with the Cu/Ag ratio obviously affect the Raman bands of the silica colloid core. The report here may supply a new technique to effectively modify the surface plasmon resonance.

Keywords: Ag–Cu alloy

1. Introduction

When the wavelength of the incident light is tuned close to the plasma resonance, conduction electrons in metal surface are excited into an extended surface electronic excited state called a surface plasmon resonance (SPR). SPR has been widely investigated for its extensive applications in phase-contrast microscopy, spatial light modulation, enhancement of an electric field, absorption measurement, radiation force to evanescent waves, generation of second harmonic waves, energy transfer in a solar cell, fluorescence spectroscopy, evanescent-wave holography [1], refractive index or dielectric constant sensor, biosensor [2], controlling nanoparticle growth [3], and surface enhanced Raman scattering (SERS) effect [4–7]. The tuning of SPR in intensity and wavelength is desired for the applications of SPR [8–10].

The layered nanoparticle with a dielectric core and a metallic nanoshell, known as a metal nanoshell, provides a tunable geometry in which the surface plasmon wavelength at the nanoshell surface can be precisely controlled by varying the core/shell ratio. For example, the surface plasmon resonance of a silica core-gold shell nanoshell can be varied over hundreds of nanometers in wavelength, across the visible and into the infrared region of the spectrum [9,10]. Recently, the studies of the plasmon energies of the concentric metal nanoshell structure supply us a new technique to manipulate the surface plasmon resonance [11]. In the concentric metal nanoshell structure, when the thickness of the interlayer spacing between the inner and outer nanoshell is small enough, the coupling strength and the energy between the plasmons on the inner and outer shell are strong, and the resulting plasmon energy differs dramatically from the isolated shell plasmons. It is also very interesting to reduce the interlay spacing to atomic level and replace the inner and outer shell of the concentric nanoshell with different kinds of metal, namely, alloy, and control the resulting surface plasmon by varying the alloying component.

In this report, the Ag–Cu alloy with controllable Cu/Ag ratio has been successfully deposited on silica colloids in order to explore the possibility of modifying the SPR by varying the metal nanoshell composition. The Ag–Cu alloy is chosen as a coating shell because Ag and Cu have a strong plasmon absorption band which lies in the visible

*Corresponding author. Fax: +86 25 8359 5535.
E-mail address: zhangjh@nju.edu.cn (J. Zhang).

0022-4596/$ - see front matter © 2007 Elsevier Inc. All rights reserved.
doi:10.1016/j.jssc.2007.01.035

region of the electromagnetic spectrum [12] that can be easily detected. In addition, the plasmon resonance absorption band of Ag colloid is stronger and sharper in comparison with Cu colloid, and occurs at shorter wavelengths. The collective plasmon resonance absorption band of the Ag–Cu alloy colloids will be easily distinguished from that of Ag or Cu colloids. This would enable us to explore the coupling between the plasmons of Ag and Cu, and find a new technique to effectively modify the SPR.

2. Experimental details

The as-prepared silica colloids [13] with average diameter of 500 nm were seeded with silver nanoparticles at first by the electroless plating approach [9]. In brief, 20 ml freshly prepared $[Ag(NH_3)_2]^+$ ions (0.1 M) solution was added into 80 ml as-prepared silica colloids suspension containing 1% PVP under stirring. The $[Ag(NH_3)_2]^+$ ions were absorbed onto the colloids surface by the negatively-charged Si–OH groups through electrostatic attraction. The negatively-charged Si–OH groups are the origin of the surface charge to protect colloids from aggregation. After 30 min, the colloids were washed with ethanol by centrifugation and ultrasonic dispersion to remove the excessive $[Ag(NH_3)_2]^+$ ions, and dispersed in ethanol solution (80 ml). Subsequently, 0.5% KBH_4 solution (10 ml) was added quickly to reduce the $[Ag(NH_3)_2]^+$ ions absorbed on the colloids surface to seed the silica colloids. The color of the solution turned from white to light brown at once. After 30 min, the colloids were washed with distilled water to remove the excessive KBH_4, and the silica colloids seeded with Ag nanoparticles were obtained. Methanol (10 ml), 0.5 g $CuSO_4 \cdot 5H_2O$, 2.5 g $NaKC_4H_4O_6 \cdot 4H_2O$, and 0.4 g NaOH were dissolved in turn in 20 ml distilled water, then the solution was added into 30 ml ethanol solution containing ~0.25 g silica colloids after seeding under stirring. After 2 min, 1 ml formaldehyde was added to alloy Cu into Ag nanoparticles for one hour. During the alloying reaction process, Cu^{2+} ions were reduced into Cu through the following reaction:

$$CuSO_4 + 3NaOH + HCHO \xrightarrow[NaKC_4H_4O_6]{\text{Ag nanoparticles}} Cu + Na_2SO_4 + HCOONa + 3H_2O.$$

In the reaction, Ag nanoparticles work as the catalyst for the formation of Cu, and the formation of Cu_2O is suppressed. Even if trace Cu_2O appears in solution, most of them will be reduced further into Cu due to the catalyst effects of Ag nanoparticles. When the binary metallic particles size reduces to nanoscale, the diffusion between the two metals is enhanced greatly, and the spontaneous alloying appears [14–16]. Here, the catalyst role and nanoscale size of Ag particles make the diffusing of Cu in Ag nanoparticles easy, and lead to the formation of Ag–Cu alloy. The Cu alloying reaction step was repeated to increase the Cu component in the alloy shell. Finally, the composite particles were washed with ethanol by centrifugation and ultrasonic dispersions.

Transmission electron microscopy (TEM) was performed on a Hitachi Model H-800 transmission electron microscope operated at 120 kV. Sample colloids were placed on a carbon-coated copper grid. Scanning electron microscopy (SEM) was performed on a LEO1530VP scanning electron microscope. Energy-dispersive X-ray analysis (EDX) was performed with a LEO153VP scanning electron microscope. X-ray photoemission spectroscopy (XPS) measurements were performed using Mg$K\alpha$ radiation (VG-ESCALAB-MK-II). The accuracy of the measured electron energies was ± 0.055 eV. Quantification of the elemental concentrations was accomplished by correcting photoelectron peak intensities for their cross sections. X-ray diffraction (XRD) was carried out on a Rigaku D/max-RA X-ray diffraction meter with Cu$K\alpha$ radiation ($\lambda = 1.5418$ Å). Raman spectra were measured with a Spex 1403 Raman spectrometer. All the spectra were recorded under identical experimental conditions: 488 nm excitation line of an argon laser, power 5 mW at the sample, three accumulations of 120 s counting time each. For the measurements of XRD, SEM, XPS, and Raman spectra, the sample thin films were prepared as follows. A few drops of suspension were spread onto a glass substrate, and dried under the protection of nitrogen gas. Transmission spectra were recorded on a U-3410 spectrophotometer. Sample colloids were diluted with ethanol for the measurements. Quartz cells with about 1-mm path length were used in the experiment.

3. Results and discussion

Fig. 1 shows the typical TEM and SEM images of the silica colloids at different stages of the coating process. As seen in Fig. 1a, compared with the pure silica colloids (see inset), the surface of the silica colloids after seeding process was uniformly covered by Ag nanoparticles with average diameter of ~7 nm. After one times Cu alloying reaction, both the coverage and size of the metal nanoparticles (~11 nm) on the silica core increased, and the shell thickness increased to ~12 nm (Fig. 1b). The second Cu alloying reaction further increased the size and shell thickness of the metal nanoparticle to ~15 and ~16 nm (Fig. 1c), respectively. After the third Cu alloying reaction, the shell thickness increased to ~ 22 nm (Fig. 1d), but was still too thin to sustain the dissolution of the silica core. As seen in Fig. 1e, most of the hollow Ag–Cu alloy spheres obtained by dissolving the silica core using HF acid were broken and aggregated together. Due to the coalescence of the seeds during the seeding growth process [9,10], the metal nanoparticles tended to be heterodisperse. Some

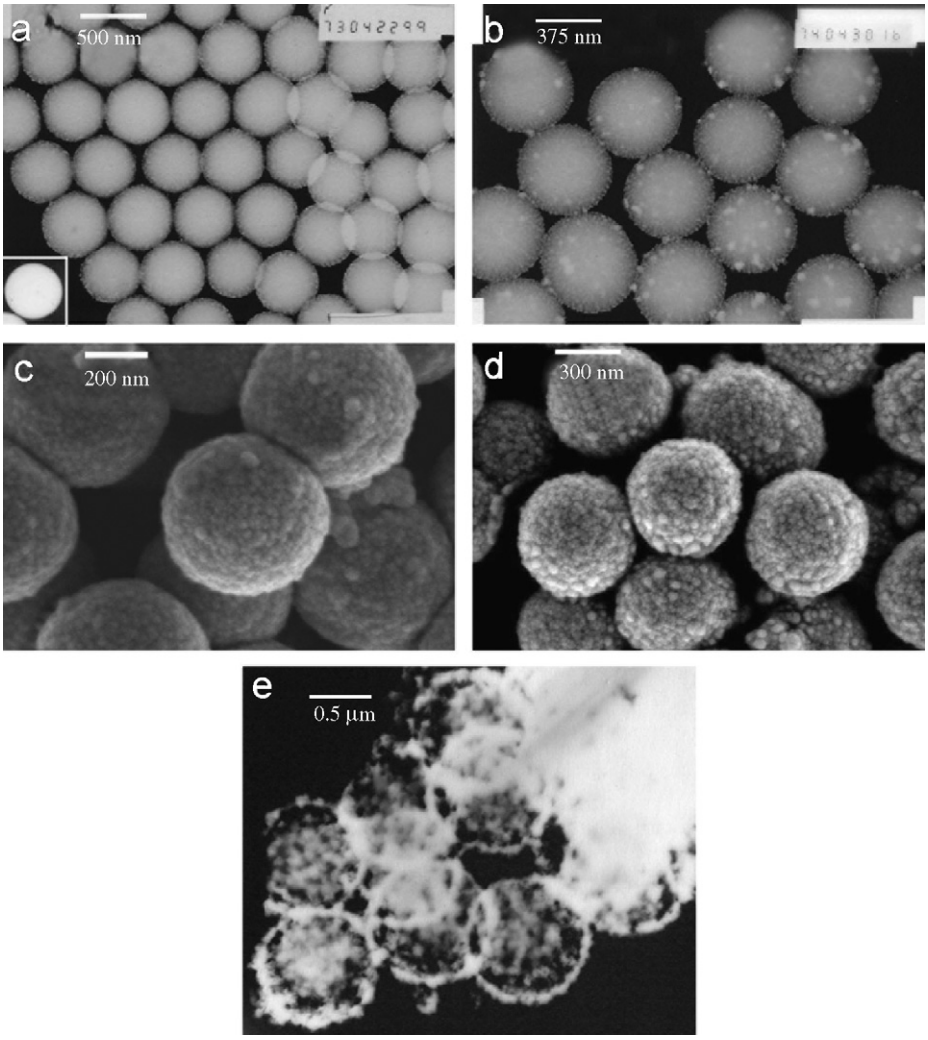

Fig. 1. TEM and SEM images of the composite particles synthesized at different stages: (a) silica colloids after Ag nanoparticles seeding, inset shows the pure silica colloids before seeding; (b)–(d) silica colloids seeded with Ag after one, two, and three times Cu alloying reactions, respectively; (e) sample of (d) after the dissolution of the silica core.

large particles with diameter of ~30 nm were observed on the composite colloids after three times Cu alloying reactions (Fig. 1d).

To ascertain the components in the composite particles, XPS measurements were made with the result shown in Fig. 2. It is seen that by increasing the Cu alloying reaction times, both the Ag 3*d* and Cu 2*p* XPS peaks shift gradually to low binding energies. The Cu/Ag atomic ratio calculated from the ratio of the integral of the Cu 2*p* and Ag 3*d* XPS peak spectra increases from 0 via 0.378, 0.599 to 0.977. The maximum shift is about 0.3 eV and 0.5 eV for the Ag 3*d* and Cu 2*p* peaks, respectively. The fact that both the Ag 3*d* and Cu 2*p* peaks show a gradual shift rather than jumping to a lower binding energy with the increase in Cu component strongly suggests that Cu is alloyed into Ag nanoparticles rather than simply deposited on the Ag nanoparticles surface during the Cu alloying reaction. In addition, the energy differences between the $3d_{5/2}$ and $3d_{3/2}$ for Ag (6.0 eV) as well as between 2 $p_{3/2}$ and $2p_{1/2}$ for Cu (19.8 eV) remain unvaried during all the Cu alloying reactions, and are exactly the same as the values of zero valent Ag and Cu [17,18]. This suggests that Ag and Cu in the coated shell of the composite particles exist in zero valent state. It is worth noting that the shoulder peaks at $2p_{3/2}$ and $2p_{1/2}$ of Cu may arise from the small amount of Cu_2O because the peaks at $2p_{3/2}$ and $2p_{1/2}$ arising from Cu in Cu_2O are slightly larger in binding energies than those originating from element Cu [17,18]. The impurity such as Cu_2O might arise from the oxidation of Cu in air because that air exposure of the surface of the samples was unavoidable while transferring the samples from solution to glass substrate for XPS measurements [18].

The element composition in the coated shell was further investigated by EDX. As shown in Fig. 3a, Ag peaks besides the Si and O peaks arising from the silica core were observed in the silica colloids seeded with Ag nanoparticles, indicating that Ag was successfully deposited on the silica colloids. With increasing the shell thickness from 12 nm via 16 to 22 nm by the Cu alloying reactions, Cu peaks appeared and increased in intensity in comparison

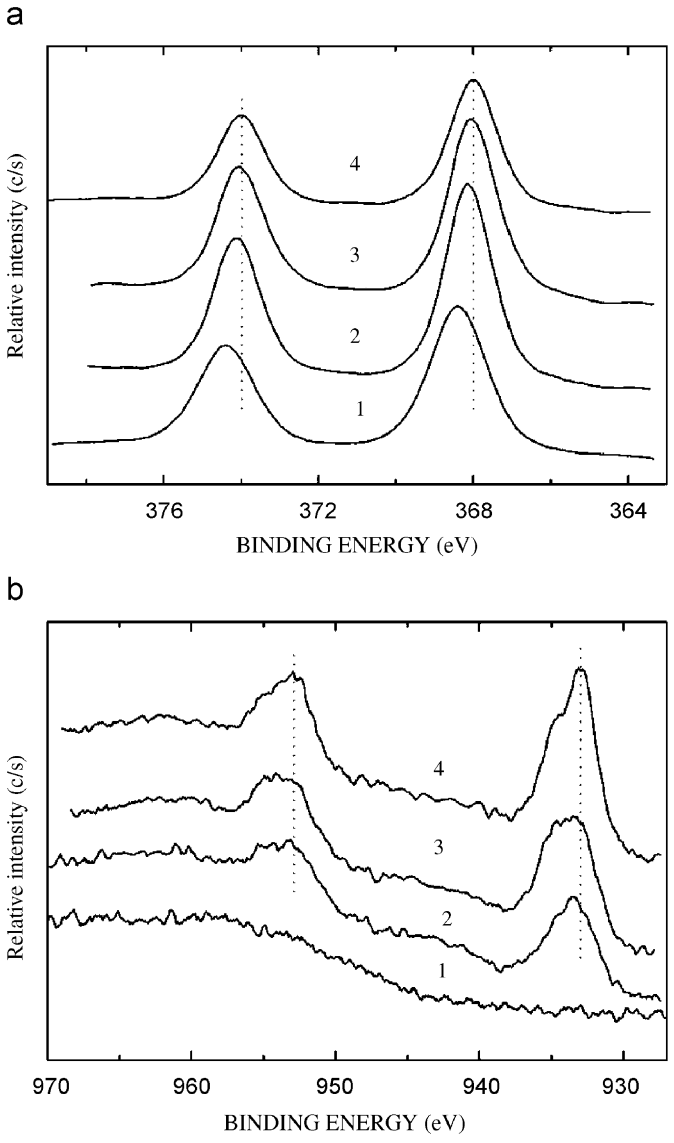

Fig. 2. XPS spectra of Ag 3*d* (a) and Cu 2*p* (b) regions for the composite particles synthesized at different stages: (1) silica colloids after Ag nanoparticles seeding, (2)–(4) silica colloids seeded with Ag after one, two, and three times Cu alloying reactions, respectively.

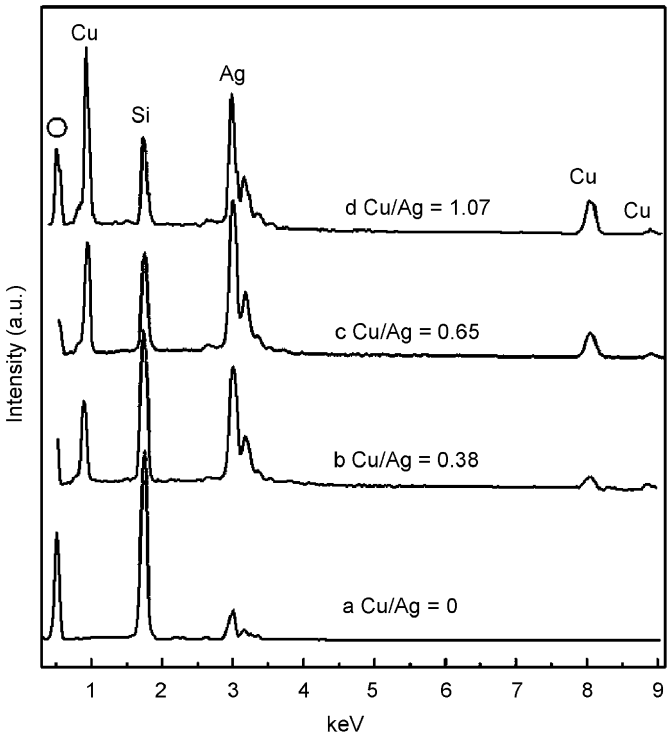

Fig. 3. EDX spectra for the composite particles synthesized at different stages: (a) silica colloids after Ag nanoparticles seeding; (b)–(d) silica colloids seeded with Ag after one, two, and three times Cu alloying reactions, respectively.

with the Ag peaks, and the Cu/Ag atomic ratio increases from 0.38 via 0.65 to 1.07 (see Fig. 3c–d). These results are similar to those obtained by the XPS spectra.

The XRD was performed to ascertain the crystal structure of the coated shell on the composite particles. As seen in Fig. 4a, the diffraction peaks of Ag for the silica colloids after seeding are very weak due to the low mol ratio of Ag/SiO_2 (see curve 1). The diffraction of Ag is barely discernable under the strong scattering background from the amorphous silica colloids that exhibit a broad peak in the small diffraction angle region. As shown in curve 2–4, the Cu alloying reactions do not cause any diffraction peaks of element or compound of Cu, but enhance the Ag diffraction peaks and make these peaks gradually discernable and strong. The increase in intensity of the diffraction peaks should arise from the increase in the metal crystallite size confirmed by SEM and TEM images. In order to clearly show the influences of the Cu alloying reactions on the XRD patterns, the expanded region (37.7–38.6° 2θ) around the strongest (1 1 1) diffraction peak for all the samples are compiled in Fig. 4b. As seen in the figure, with the increase of the Cu alloying reaction times, the (1 1 1) peak gradually shifts to high 2θ-degree, thus indicating the formation of the Ag–Cu alloy. These analyses as well as the XPS results clearly indicate that Ag–Cu alloy is successfully deposited on the silica core.

The UV–vis absorption spectra were recorded for the composite particles to analysis the SPR character, which are shown in Fig. 5. The silica colloids seeded with Ag nanoparticles have a broad absorption peak around 456 nm (see curve a), which arises from the SPR of Ag nanoparticles [9,10,12]. After performing one times Cu alloying reaction, the SPR peak red shifts to 470 nm with a great increase in intensity. A second peak around 585 nm originating from the Cu SPR [12,19–21] appears as a shoulder. By increasing the Cu alloying reaction times and thus the Cu/Ag ratio, both the SPR absorption peaks of Ag and Cu become increased in intensity, narrowed, blue shifted, and tend to merge into a single absorption peak. According to the previous reports [12,19,20], the formation of one single absorption suggests that the Cu–Ag alloy is formed during the Cu alloying reactions. Furthermore, if Cu–Ag alloy is not formed and element Cu is simply

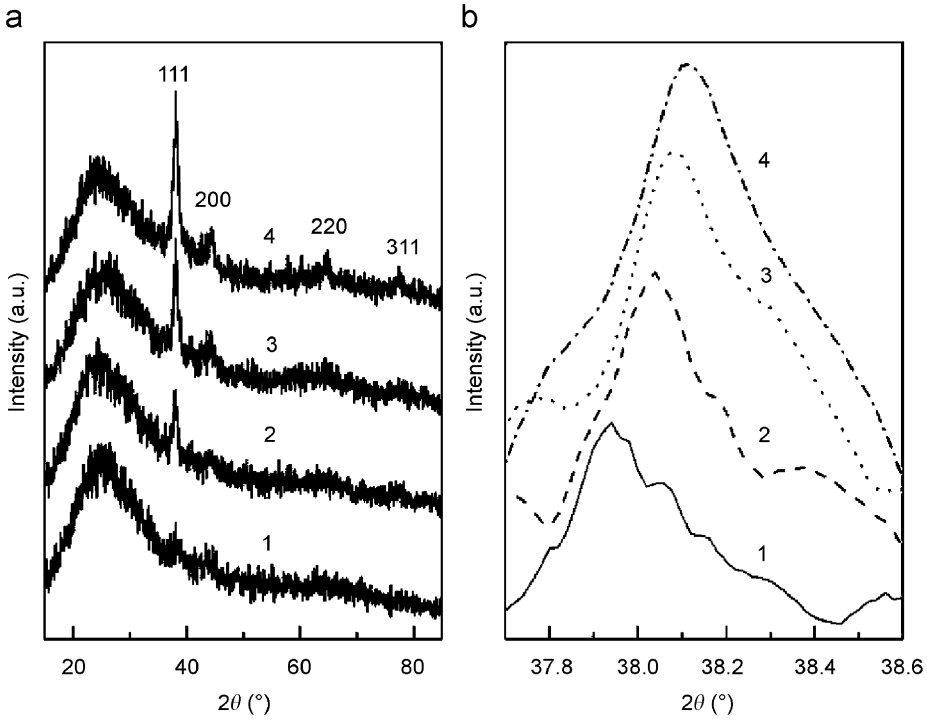

Fig. 4. XRD patterns (a) of the composite particles synthesized at different stages: (1) silica colloids after Ag nanoparticles seeding, (2)–(4) silica colloids seeded with Ag after one, two, and three times Cu alloying reactions, respectively. The corresponding expanded region (37.7–38.6° 2θ) around the (1 1 1) diffraction peak for all the samples are compiled in (b).

deposited on the Ag nanoparticles in the coating process, with increased Cu/Ag ratio, the Ag SPR band should be depressed but not shift, and the Cu SPR band should increase in intensity and red shift [12]. This is ruled out by the experimental results.

Since most of the nanoparticles deposited on the silica core are smaller than 20 nm in our samples, the absorption is reasonably described by Mie scattering theory in the electric dipole approximation [12,19,22] and is given by

$$\alpha = 18\pi n_d^3 p\varepsilon_2/\lambda[(\varepsilon_1 + 2n_d^2)^2 + \varepsilon_2^2], \quad (1)$$

where α is the absorption coefficient, $\varepsilon(\lambda) = \varepsilon_1 + i\varepsilon_2$ is the dielectric constant of the metal, p is the volume fraction of the metal particles and n_d is the index of refraction of the dielectric host. The absorption is expected to exhibit a peak at the surface plasmon resonance frequency for which the condition $\varepsilon_1 + 2n_d^2 = 0$ is met. Beyond 354 nm in wavelength, the real part of the dielectric constants of both Ag and Cu decreases with increasing wavelength, and ε_1(Cu) is larger than ε_1(Ag) [23]. The alloying of Cu into Ag nanoparticles will increase ε_1 and make the SPR peak red shifted. The increase of particles size due to Cu alloying reaction may also lead to a small red shift (<5%) of the position of the SPR [22]. These, as well as the increase of the shell coverage and thickness [9,10], collectively lead to the red shift of the Ag SPR absorption peak caused by the first times Cu alloying reaction as shown in Fig. 5b.

From Eq. (1), the intensity of the SPR is inversely related to ε_2; the alloying Cu into Ag nanoparticles will increase ε_2 and thus decrease the SPR intensity because ε_2(Cu) is larger than ε_2(Ag) beyond 200 nm in the wavelength of interest [23]. However, as shown in Fig. 5, the SPR bands are enhanced and narrowed with the alloying Cu, and begin to blue shift and merge into a single band after two times of Cu alloying reactions. Although the increases of particles' size and coverage caused by the Cu alloying can account for the increased intensity and the narrowing effect of the SPR bands [9,10], the large blue shift of the SPR bands is still an open question.

As reported by Magruder et al. [19] with increasing the degree of alloying, the SPR band of the Ag–Cu composite particles doped silica film red shifts and decreases in intensity. However, with increasing Cu concentration in the Ag–Cu alloy particles, the SPR blue shifts and decreases in intensity [20]. In the Ag–Cu mixture nanoclusters doped silica glass films [21], with the increase in Cu component, the blue shift and decrease in intensity of both Cu and Ag SPR bands have also been observed. All the above blue shifts have been ascribed to an interaction between Ag and Cu. Considering the report of Prodan et al. [11], the blue shifts of the SPR bands induced by the second and third times Cu alloying reactions can be ascribed to the SPR coupling between Cu and Ag. Here the abnormal increase in intensity of the SPR bands caused by the Cu alloying reactions in comparison to the reported results [19–21] should mainly originate from the increase of the shell thickness [9,10]. According to the above results and discussion, the goal coupling between the plasmons on the inner and outer shell at atomic level in the concentric metal nanoshell structure has been realized here to a

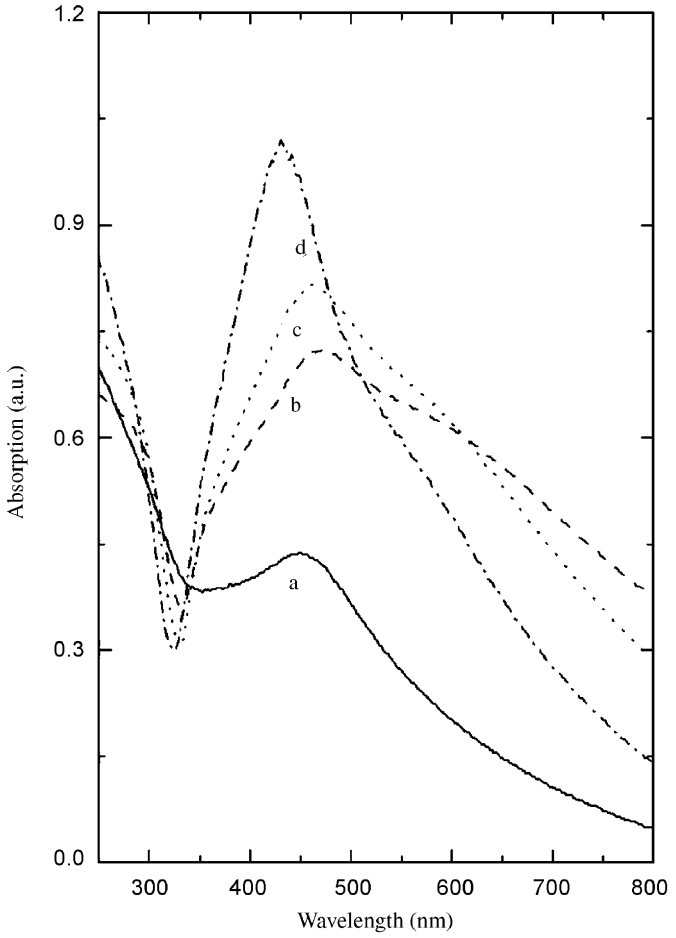

Fig. 5. Absorption spectra of the composite particles synthesized at different stages: (a) silica colloids after Ag nanoparticles seeding; (b)–(d) silica colloids seeded with Ag after one, two, and three times Cu alloying reactions, respectively.

certain degree by coating the silica colloids with the Cu–Ag alloy. The collective plasmon resonance of Cu–Ag alloy differs dramatically from that of Ag or Cu, and can be easily tuned in wavelength by changing the Cu/Ag ratio. Furthermore, the unique core-shell structure provides us a new technique to modify the SPR intensity of the Cu–Ag alloy by varying the alloy shell thickness.

As seen from Fig. 4, the silica colloids core used here is amorphous silica which usually has two broad Raman bands [24–26]. One is located around 460 cm^{-1}, and is attributed to the symmetric bending motion of the Si–O–Si linkages. The other band is located around 1000 cm^{-1}, and originates from the asymmetric stretching of the bridging oxygen. Currently, local electromagnetic field enhanced by the excitation of surface plasmons at the metal surface is widely believed to be responsible for the surface enhanced Raman scattering (SERS) effect [5–8]. An enhancement of SERS effect can be maximized when the SPR wavelength is equal to the average value of the excitation and Raman scattering wavelengths [6]. With the 488 nm excitation line of an argon laser used in our experiments, the Stokes bands around 460 and 1000 cm^{-1} of amorphous silica are located, on the wavelength scale, at approximately 499.2 and 513.0 nm, respectively. So the SPR peaks located at 493.6 and 500.5 nm (calculated from the equation $(\lambda_{\text{excitation line}} + \lambda_{\text{Raman scattering}})/2$ [6]) are expected to give maximum contribution to the enhancement for the Raman bands at 460 and 1000 cm^{-1}, respectively. As shown in Fig. 5, the SPR bands position in all the composite particles is closed to the expected SPR bands for the maximum enhancement. Furthermore, the SPR peaks become enhanced in intensity by the Cu alloying reaction. These motivate us to investigate whether the variations of the SPR intensity with Cu component can affect the Raman bands of the silica core, namely, whether the SERS effect can be found in the composite colloids system itself.

As shown in Fig. 6a, two broad Raman bands around 460 and 1000 cm^{-1} were observed for the thin film made of the silica colloids seeded with Ag nanoparticles. The alloying Cu into Ag nanoparticles by the first time Cu alloying reaction enhances the SPR intensity, and obviously enhances the two Raman bands (curve b). Further increasing the SPR intensity by the second time Cu alloying reaction not only further enhances the two Raman bands, but also leads to a new Raman band around 790 cm^{-1} (Fig. 6c). The new band arises from a Si–O stretching vibration that contains considerable motion of the silicon atom [26]. The third time Cu alloying reaction continuously enhances the SPR band and the Raman bands around 460 and 790 cm^{-1}, but greatly blue shifts the SPR band to 431 nm and weakens the Raman band around 1000 cm^{-1} (Fig. 6d), which can be ascribed to the large deviation between the actual SPR position and the expected SPR position (500.5 nm) for the maximum enhancement. It should be noted that the above investigation about the SERS effect of the composite colloids

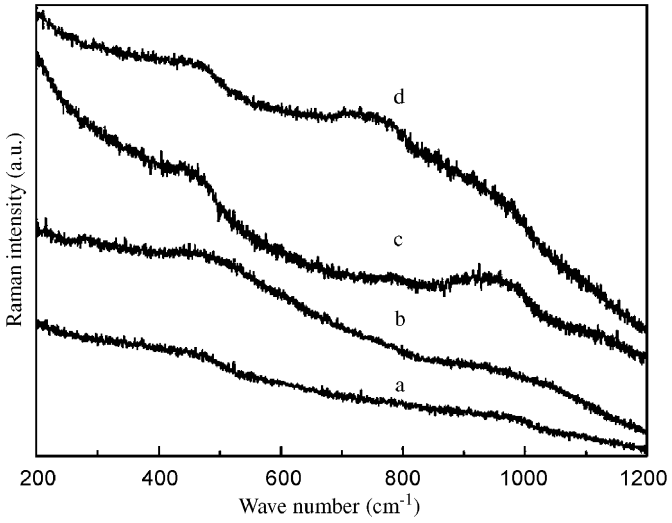

Fig. 6. Raman spectra of the thin films made of the composite particles synthesized at different stages: (a) silica colloids after Ag nanoparticles seeding; (b)–(d) silica colloids seeded with Ag after one, two, and three times Cu alloying reactions, respectively. The spectra are vertically shifted for clarity.

system itself is qualitative because there might be a high proportion of re-absorption within the alloy shell surrounding the silica core.

4. Conclusion

In summary, the possibility of modifying the plasmon resonance at the nanoshell surface through varying the metal nanoshell composition has been investigated by fabricating the silica@Ag–Cu alloy core-shell composite colloids for the first time. It was found that varying the Cu/Ag ratio of the alloy nanoshell has obvious influences on the surface plasmon resonance of the composite colloids and the Raman bands of the amorphous silica core.

Acknowledgments

J.H. Zhang acknowledges Project 10404013 supported by NSFC, and H. Dong, P. Zhan, and X.N. Zhao for their help in the SEM measurements.

References

[1] S. Maruo, O. Nakamura, S. Kawata, Appl. Opt. 36 (1997) 2343.
[2] E. Fujii, T. Koike, K. Nakamura, S. Sasaki, K. Kurihara, D. Citterio, Y. Iwasaki, O. Niwa, K. Suzuki, Anal. Chem. 74 (2002) 6106.
[3] R. Jin, Y.C. Gao, E. Hao, G.S. Métraux, G.C. Schatz, C.A. Mirkin, Nature 425 (2003) 487.
[4] M. Moskovits, Rev. Mod. Phys. 57 (1985) 783.
[5] K. Kneipp, Y. Wang, H. Kneipp, L.T. Perelman, I. Itzkan, R.R. Dasari, M.S. Feld, Phys. Rev. Lett. 78 (1997) 1668.
[6] N. Félidj, J. Aubard, G. Lévi, J.R. Krenn, M. Salerno, G. Schider, B. Lamprecht, A. Leitner, F.R. Aussenegg, Phys. Rev. B 65 (2002) 075419.
[7] J.B. Jackson, S.L. Westcott, L.R. Hirsch, J.L. West, N.J. Halas, Appl. Phys. Lett. 82 (2003) 257.
[8] C. Jiang, S. Markutsys, V.V. Tsukruk, Langmuir 20 (2004) 882.
[9] J. Zhang, J. Liu, S. Wang, P. Zhan, Z. Wang, N. Ming, Adv. Funct. Mater. 14 (2004) 1089.
[10] S.J. Oldenburg, R.D. Averitt, S.L. Westcott, N.J. Halas, Chem. Phys. Lett. 288 (1998) 243.
[11] E. Prodan, C. Radloff, N.J. Halas, P. Nordlander, Science 302 (2003) 419.
[12] P. Mulvaney, Langmuir 12 (1996) 788.
[13] J.H. Zhang, P. Zhan, Z.L. Wang, W.Y. Zhang, N.B. Ming, J. Mater. Res. 18 (2003) 649.
[14] H. Yasuda, H. Mori, M. Komatsu, K. Takeda, J. Appl. Phys. 73 (1993) 1100.
[15] H. Yasuda, H. Mori, Phys. Rev. Lett. 69 (1992) 3747.
[16] T. Shibata, B.A. Bunker, Z. Zhang, D. Meisel, C.F. Vardeman, J.D. Gezelter, J. Am. Chem. Soc. 124 (2002) 11989.
[17] J.F. Moulder, W.F. Stickle, P.E. Sobol, K.D. Bomben, in: J. Chastain Jr., R.C. King (Eds.), Handbook of X-ray Photoelectron Spectroscopy, Physical Electronics, Inc., Eden Prairie, MN, 1995, pp. 86–120 (Chapter II).
[18] Á. Molnár, I. Bertóti, J. Szépvölgyi, G. Mulas, G. Cocco, J. Phys. Chem. B 102 (1998) 9258.
[19] R.H. Magruder III, J.E. Wittig, R.A. Zuhr, J. Non. Cryst. Solids 163 (1993) 162.
[20] R.H. Magruder III Jr., D.H. Osborne, R.A. Zuhr, J. Non. Cryst. Solids 176 (1994) 299.
[21] G. De Tapfer L., M. Catalano, G. Battaglin, F. Caccavale, F. Gonella, P. Mazzoldi, R.F. Haglud Jr., Appl. Phys. Lett. 68 (1996) 3820.
[22] U. Kreibig, L. Genzel, Surf. Sci. 156 (1985) 156.
[23] P.B. Johnson, R.W. Christy, Phys. Rev. B 6 (1972) 4370.
[24] P. Colomban, C. Truong, Raman Spectrosc. 35 (2004) 195.
[25] P. Gangopadhyay, R. Kesavamoorthy, K.G.M. Nair, R. Dhandapani, J. Appl. Phys. 88 (2000) 4975.
[26] C.H. Polsky, K.H. Smith, G.H. Wolf, J. Non. Cryst. Solids 248 (1999) 159.